PNAS RESEARCH ARTICLE | DEVELOPMENTAL BIOLOGY

Transdifferentiation occurs without resetting development-specific DNA methylation, a key determinant of full-function cell identity

Ahmed Radwan[a,1], Jason Eccleston[b,c,1], Ofra Sabag[a], Howard Marcus[a], Jonathan Sussman[b,c], Alberto Ouro[a], Moran Rahamim[a], Meir Azagury[a], Batia Azria[a], Ben Z. Stanger[b,c,2], Howard Cedar[a,2], and Yosef Buganim[a,2]

Affiliations are included on p. 8.

Contributed by Howard Cedar; received July 2, 2024; accepted August 21, 2024; reviewed by Duanqing Pei and Jay Rajagopal

A number of studies have demonstrated that it is possible to directly convert one cell type to another by factor-mediated transdifferentiation, but in the vast majority of cases, the resulting reprogrammed cells are unable to maintain their new cell identity for prolonged culture times and have a phenotype only partially similar to their endogenous counterparts. To better understand this phenomenon, we developed an analytical approach for better characterizing trans-differentiation-associated changes in DNA methylation, a major determinant of long-term cell identity. By examining various models of transdifferentiation both in vitro and in vivo, our studies indicate that despite convincing expression changes, transdifferentiated cells seem unable to alter their original developmentally mandated methylation patterns. We propose that this blockage is due to basic developmental limitations built into the regulatory sequences that govern epigenetic programming of cell identity. These results shed light on the molecular rules necessary to achieve complete somatic cell reprogramming.

plasticity | metaplasia | epigenetics | development | regulation

Significance

Many studies have shown that it is possible to convert one cell type to another using specific factors. However, these reprogrammed cells often fail to maintain their new identity for long and only partially resemble their intended type. To understand why this happens, we developed a method to analyze changes in DNA methylation, which is crucial for maintaining long-term cell identity. By studying various models, we found that reprogrammed cells struggle to change their original DNA methylation patterns. We believe that this is due to fundamental developmental limitations in the regulatory sequences that control cell identity. Our findings provide insights into the molecular requirements for fully reprogramming somatic cells.

In mammals, development takes place in a progressive manner, beginning with reprogramming of the gametic phenotype to form pluripotent cells in the early embryo and continuing through subsequent stages of differentiation into more specific cell types. In vivo, this process appears to involve built-in barriers that ensure unidirectionality and somatic cell-type stability (1). Epigenetic marks, in particular DNA methylation, play an important role in this scheme (2). Early in embryogenesis, DNA methylation patterns of the gametes are erased from almost all sites (3, 4), setting the stage for the re-establishment of a basal profile at the time of implantation, which is efficiently accomplished through a wave of genome-wide methylation (85 to 100%) in conjunction with sequence-directed protection of CpG islands (5–7). As development proceeds, each emerging cell type undergoes programmed site-specific changes in regulatory-sequence DNA methylation as an integral part of differentiation (8).

The general idea that early embryonic reprogramming is necessary for normal development has been elegantly validated by studies demonstrating the artificial reprogramming of adult somatic cells. It has been shown, for example, that unfertilized enucleated Xenopus oocytes transplanted with a tadpole nucleus are capable of generating a full adult organism (9), suggesting that factors in the oocyte cytoplasm can induce pluripotency in a manner similar to the normal process of germ-line nuclear reprogramming. Similar experiments have also been performed in mammals (10). Yamanaka identified specific master transcription factors that can reprogram multiple different mammalian somatic cell types into pluripotent embryonic stem cells which can then go on to develop into full functioning organisms with stable cell-type identity (11). This reprogramming is accompanied by re-establishment of the pluripotency methylation pattern; accordingly, embryonic stem cells have been shown to actually harbor all the dynamic molecular machinery required for this process (12).

Another approach to somatic-cell reprogramming is to directly transdifferentiate one specific cell type into an alternate somatic cell without first going through an early embryonic reprogramming step. This was initially accomplished by means of somatic cell-fusion and more recently through overexpression of specific master genes known to be involved in normal differentiation of the desired cell type (13, 14). Transdifferentiation may also occur in response to tissue injury in vivo (15). However, in several cases, it has been demonstrated that the newly induced cell identity fails to encompass the complete expression pattern (16) and lacks the ability to fully manifest the desired

Author contributions: A.R., B.Z.S., and Y.B. designed research; J.E., H.M., and B.A. analyzed data; O.S., J.S., A.O., M.R., and M.A. performed research; and H.C. wrote the paper.

Reviewers: D.P., Guangzhou Institutes of Biomedicine and Health; and J.R., Massachusetts General Hospital.

The authors declare no competing interest.

[1]A.R. and J.E. contributed equally to this work.

[2]To whom correspondence may be addressed. Email: bstanger@upenn.edu, cedar@mail.huji.ac.il, or yossib@ekmd.huji.ac.il.

This article contains supporting information online at https://www.pnas.org/lookup/suppl/doi:10.1073/pnas.2411352121/-/DCSupplemental.

Published September 18, 2024.

cell type's functional spectrum. Furthermore, in numerous examples, the acquired cell identity can only be maintained in the presence of ongoing exogenous factors or injury-associated stimuli (17–20).

While it has been demonstrated that all developmental decisions involving changes in expression require accompanying alterations in DNA methylation in order to ensure long-term stability (21, 22), very little is known about the dynamics of this important epigenetic mark during the process of transdifferentiation. To address this question, we created an approach for pinpointing developmentally relevant DNA methylation dynamics and used this to analyze multiple models of transdifferentiation in vitro and in vivo. We report here that despite changes in gene expression and chromatin structure that approximate the cell state, methylation signatures remain those of the starting cell type. This inability to establish the correct cell-identity methylation profile may explain the general incomplete reprogramming of transdifferentiated cells (17).

Results

Pioneering studies carried out in the 1980s demonstrated that fibroblast nuclei can be reprogrammed to generate a myoblast phenotype by fusion with muscle cells from a different species, a transdifferentiation process mediated through the activation of master transcription factors such as MyoD (23, 24). Identifying, isolating, and introducing these factors into fibroblasts in vitro leads to the direct induction of the cellular phenotype (25, 26). Similar approaches have also been employed for the reprogramming of other cell types (14).

In this study, we infected mouse embryonic fibroblasts (MEFs) with lentivirus carrying a Dox-inducible MyoD gene. Upon

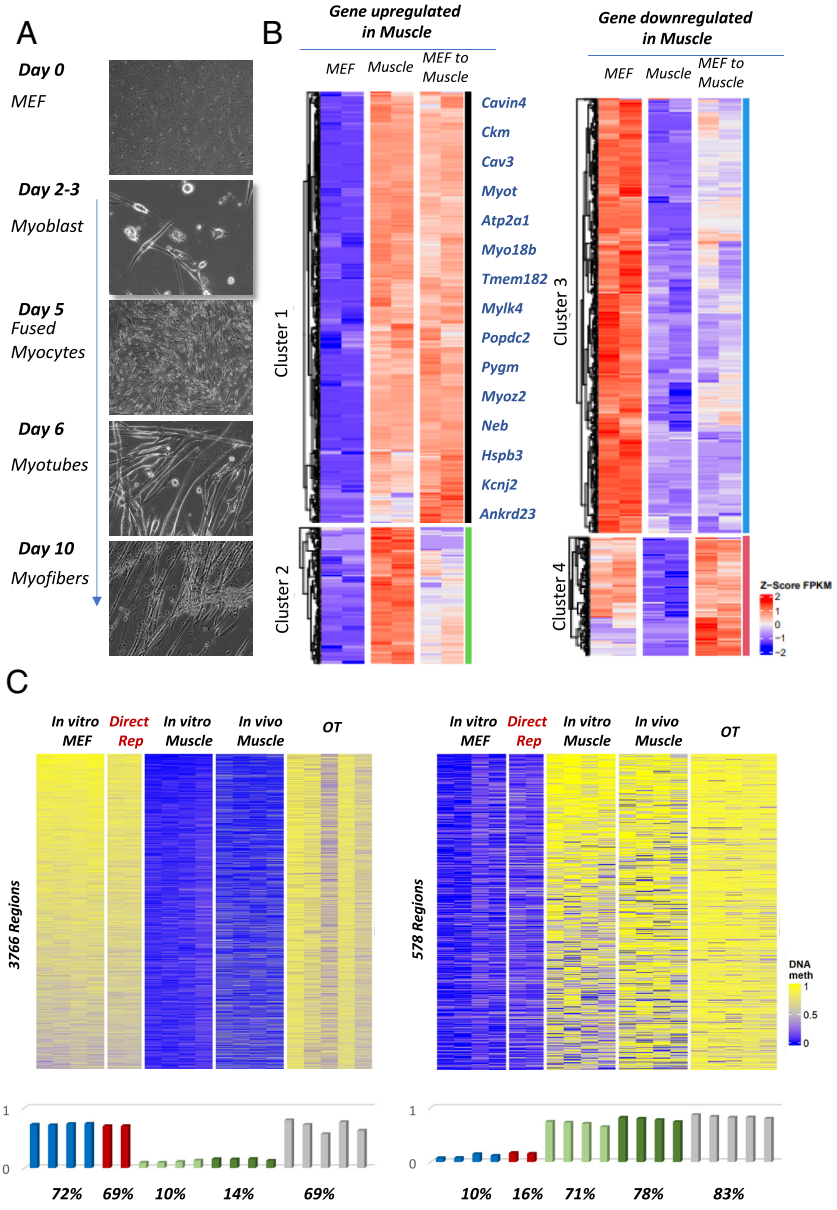

Fig. 1. Direct reprogramming from MEFs to muscle—morphology, expression, and DNA methylation. (*A*) Representative bright field images showing cell morphology during direct reprogramming process from MEF to muscle. (*B*) Expression heat map showing genes that are up-regulated (*Left*) and down-regulated (*Right*) in normal muscle cells compared to MEFs together with the expression level seen in reprogrammed cells. (*C*) Heat map and histogram (average methylation for each sample) of regions specifically undermethylated in muscle (*Left*) or in MEFs (*Right*) compared to methylation patterns seen in reprogrammed cells and in other tissues (OT) by RRBS.

induction, these cells underwent a morphological conversion to a myoblast phenotype (Fig. 1*A*). Converted cells were then isolated and subjected to RNA-Seq and the resulting transcriptional profiles were compared to those of preinduced MEFs and normal muscle stem-cell derived myoblasts. This analysis revealed that about 70% of muscle-specific genes were up-regulated while a similar percentage of fibroblast-specific genes were down-regulated (Fig. 1*B*). Thus, overexpression of MyoD causes fibroblasts to adopt many features of the myoblast phenotype at both the morphological and transcriptional levels.

We then extracted DNA from these same cellular populations and performed genome-wide CpG methylation analysis using reduced representation bisulfite sequencing (RRBS). Despite covering about 10% of all CpG sites in the genome, RRBS provides exceptionally deep coverage, enriched for sites located in regulatory regions, such as promoters and enhancers (27). These regulatory regions are demethylated in a tissue-specific manner during development, such that every cell in the body is defined by a unique regulatory-sequence methylation pattern (8, 28). Consequently, to correctly interpret the directional dynamics of methylation changes that occur during transdifferentiation and eliminate those due to cell environment, we focused exclusively on these developmentally meaningful regions (Diagram 1).

First, we compiled a library of regions specifically undermethylated in myoblasts or fibroblasts, thereby defining their methylation signature. As previously shown (28), differentially methylated regions (DMRs) are almost always associated with intra- or inter-genic regulatory sequences, with only a small percentage representing gene promoters (*SI Appendix*, Fig. S1*A*). Using these sequences as a developmental reference, we then assessed the DNA methylation status of the transdifferentiated cells. In contrast to gene expression patterns, which reflected the new cell type, the MyoD-expressing cells did not exhibit any new muscle-specific demethylation (Fig. 1*C*), even at sequences located in close association with transcriptionally induced muscle-specific genes (Fig. 1*B*). Likewise, transdifferentiation was not accompanied by any remethylation of MEF-specific enhancer regions. To confirm these findings, we used the same approach to analyze an independent dataset published by a different group (18). This revealed an identical pattern, with the transdifferentiated myoblast cells retaining the original MEF methylation profile (*SI Appendix*, Fig. S1*B*). Taken together, these studies indicate that while factor-induced transdifferentiation results in the adoption of a partially reconfigured transcriptome, this is not accompanied by developmentally significant changes in the DNA methylome, perhaps explaining why these cells have been shown to undergo incomplete reprogramming (18).

We next investigated whether this phenomenon holds true for other transdifferentiation systems. It has previously been shown that fibroblasts can be induced to transdifferentiate into phenotypically functional neurons using several different combinations of master transcription factors (29, 30). In one study, the authors carried out whole genome bisulfite sequencing (WGBS), thus obtaining the full DNA methylation pattern both in the source cells as well as the cells generated by transdifferentiation. This study revealed changes in DNA methylation dynamics on promoter regions; however, methylation changes in developmentally critical regulatory regions were not explored. Hence, we reanalyzed this dataset to determine whether the reprogramming of fibroblasts is accompanied by demethylation of neuronal progenitor cell (NPC)-specific regulatory regions. As before, methylome analysis revealed a discrepancy between gene expression and methylation patterns. Regulatory regions that are known to be specifically undermethylated in NPCs remained fully methylated upon

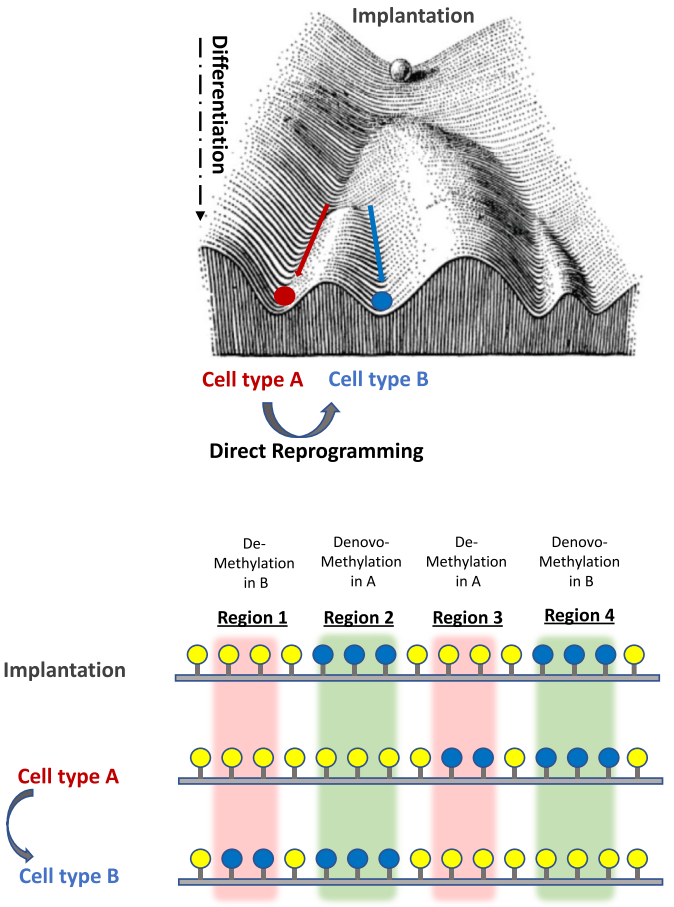

Diagram 1. Dynamics of DNA methylation during development. Conrad Waddington's epigenetic landscape. The ball represents a cell and the bifurcating system of valleys represents trajectories of cell state. This diagram by C.H. Waddington neatly encapsulates the developmental pathways and progressive divergence of cells as they differentiate in the embryo. Reproduced from Waddington © (1) George Allen and Unwin (London). The diagram shows regions of DNA from a developmental perspective. The upper row shows the methylation state of each region at the time of implantation (E6.5) and this same pattern is preserved in most tissues of the adult organism. In other words, the pattern established in the early embryo is then maintained in all tissues, with only some undergoing tissue-specific changes in cell type A or B. Methylated (Yellow), undermethylated (Blue). Region 1 is specifically demethylated in Cell-type B during development. If it does not undergo demethylation following transdifferentiation, this indicates that these cells have failed to adopt a B cell identity probably because the induction factors were unable to activate the site-specific demethylation machinery originally employed during earlier B cell development. Region 2 appears to behave in a very similar manner, but from the developmental perspective, this region is actually set up as unmethylated in the embryo and remains that way in all cells. During Cell-type A development, it becomes specifically de novo methylated—a completely different event. Thus, if the transdifferentiation event failed to demethylate this segment, it is probably because the factors and motifs necessary for specifically demethylating this region do not exist. Indeed, during normal development, this sequence never undergoes specific demethylation—because it is already unmethylated in all cell types of the body. Region 3 is specifically demethylated in Cell-type A. If it fails to become remethylated when A is transdifferentiated to B, this is probably because this type of specific event never occurs in vivo during normal development and the molecular components needed for this do not exist. Region 4 has the exact same A/B differential methylation pattern as that of region 3, but in this case, it is a result of B cell-specific de novo methylation. If this region fails to become methylated in the transdifferentiation process, it is probably because the factors used to convert A to B were unable to activate this specific de novo methylation machinery. It should be noted that, for the sake of simplicity, the analysis in this paper only includes regions of tissue-specific demethylation (e.g., regions 1 and 3).

neuronal transdifferentiation, even after extended exposure to several different neuron-specific master gene inducers (Fig. 2 *A* and *B*). The relatively preserved MEF methylation profile of the transdifferentiated neurons was again in contrast to the moderate

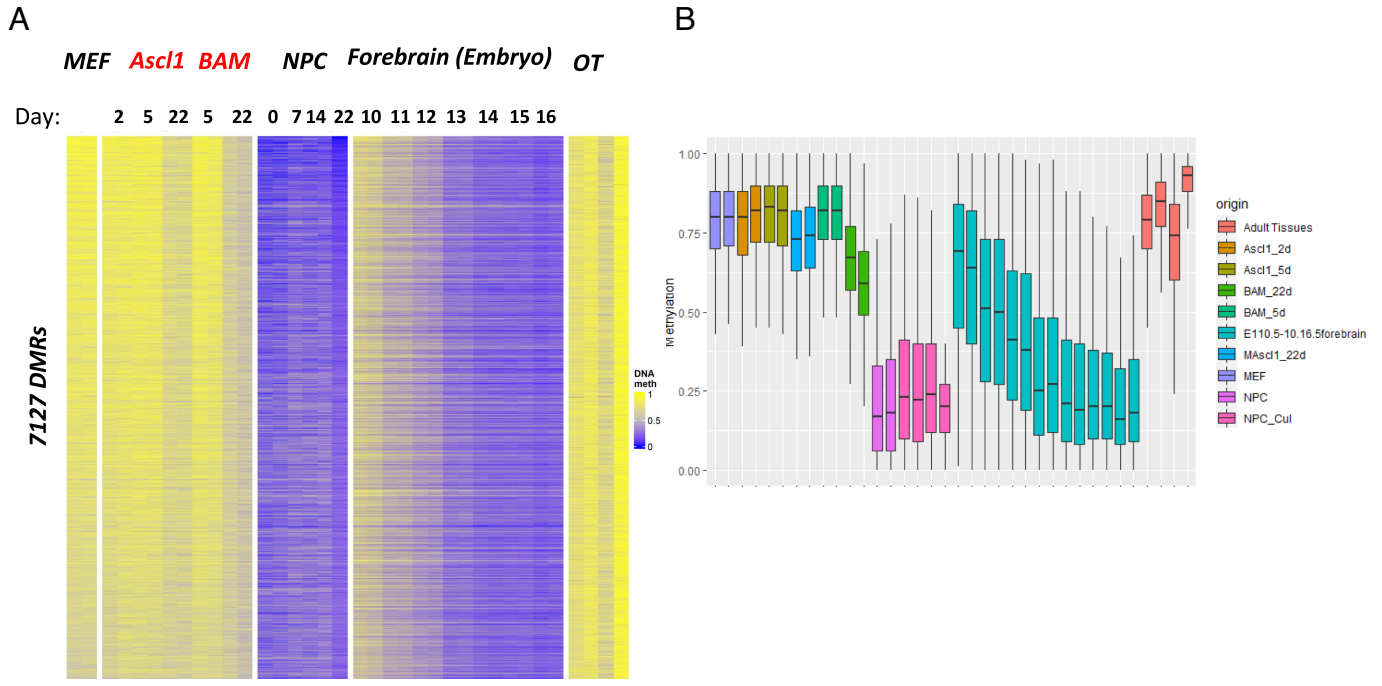

Fig. 2. Direct reprogramming from MEFs to NPC—DNA methylation. Heatmap and boxplot of regions specifically unmethylated in NPCs (*A* and *B*) as compared to those seen in MEFs reprogrammed to NPCs following direct reprogramming for various times using either the Ascl1 or BAM inducers in forebrain (E10–E16) and in OT by WGBS. Their state of methylation is also shown for different stages of forebrain development (E10–E16), as well as in OT.

gene expression changes consistent with an emerging neuronal phenotype.

Finally, we asked how methylation patterns change in the setting of transdifferentiation in vivo. It is increasingly appreciated that changes in cell identity occur as a physiological response to tissue injury in multiple organs (15), with the conversion of hepatocytes to cholangiocyte-like cells (biliary epithelial cells: BECs) in the liver serving as one of the best examples (31, 32). In one of our earlier studies, we have demonstrated that these same Hepatocyte-derived BECs exhibit a gene expression pattern (RNA-Seq) and chromatin configuration (ATAC-seq) that partially resembles that of bona fide BECs (33).

As before, we began by generating a library of developmentally associated regulatory regions from control (untreated) hepatocytes or BECs. Then, to induce hepatocyte-to-BEC transdifferentiation, we fed mice a diet containing 0.1% 3,5-diethoxycarbonyl-1,4 dihydrocollidine (DDC) and used flow cytometry to isolate the reprogrammed cells based on the dual expression of a hepatocyte-lineage marker (YFP) and a BEC marker (EpCAM) (see *Materials and Methods* for details). As a control for the injury condition itself, we also isolated hepatocytes and BECs from the DDC-treated mice. Finally, we compared the methylation pattern of the transdifferentiated cells to those of purified injured and uninjured hepatocytes and BECs.

Consistent with our in vitro results, we found that despite partial remodeling of the transcriptome in the transdifferentiated BECs, there was no significant reconfiguration of the overall methylome (*SI Appendix*, Fig. S2*A*). Hepatocyte-specific regulatory loci remained in their methylated conformation (Fig. 3*A*), while cholangiocyte-specific regions retained their undermethylated state, even though these sites are normally methylated in hepatocytes (Fig. 3*B*). These clear-cut findings may help explain why these injury-induced cholangiocyte-like cells are unstable, undergoing reversion to hepatocytes once the injury stimulus is removed or upon transplantation to healthy recipients (17).

Despite the lack of DNA methylation changes, we were interested to see whether transdifferentiation is accompanied by alterations in chromatin structure. To this end, we assayed for transposase-accessible with sequencing (ATAC-Seq) using data obtained from the transdifferentiated cells and compared this map to that seen in normal hepatocytes and cholangiocytes. While the cholangiocyte-specific demethylated regions are, as expected, packaged in a highly accessible form in these cells, these same regulatory sites are in an inaccessible conformation in hepatocytes, where they are methylated. These sites, however, do undergo considerable structural changes, becoming more accessible in the transdifferentiated cells (Figs. 3*C* and 4 and *SI Appendix*, Fig. S2*B*). This indicates that these regulatory regions are indeed utilized and further explains how the genes associated with these loci undergo activation, thereby generating the cholangiocyte-like phenotype. Similar results were also observed when we analyzed data obtained for the conversion of MEFs to myoblasts (*SI Appendix*, Fig. S3). Taken together, these results suggest that the changes in gene expression and chromatin structure associated with transdifferentiation of one somatic cell type into another can occur in the absence of developmentally mandated changes in DNA methylation both in vitro and in vivo.

As opposed to all these direct transdifferentiation experiments, which fail to recapitulate appropriate DNA methylation patterns, somatic cells converted to trophoblast stem cells (34, 35) or induced to pluripotency undergo near complete epigenetic reprogramming, with specifically hypomethylated enhancer-associated CpG sites from the original somatic cells becoming remethylated, while any sites that underwent programmed de novo methylation during differentiation return to their hypomethylated state (35, 36). Indeed, this factor-mediated pluripotency reprogramming has been shown to accurately (99%) regenerate both the expression and epigenetic patterns of this early stage in development (37).

In light of these findings, we decided to employ a more conventional approach for generating NPCs from MEFs, using a

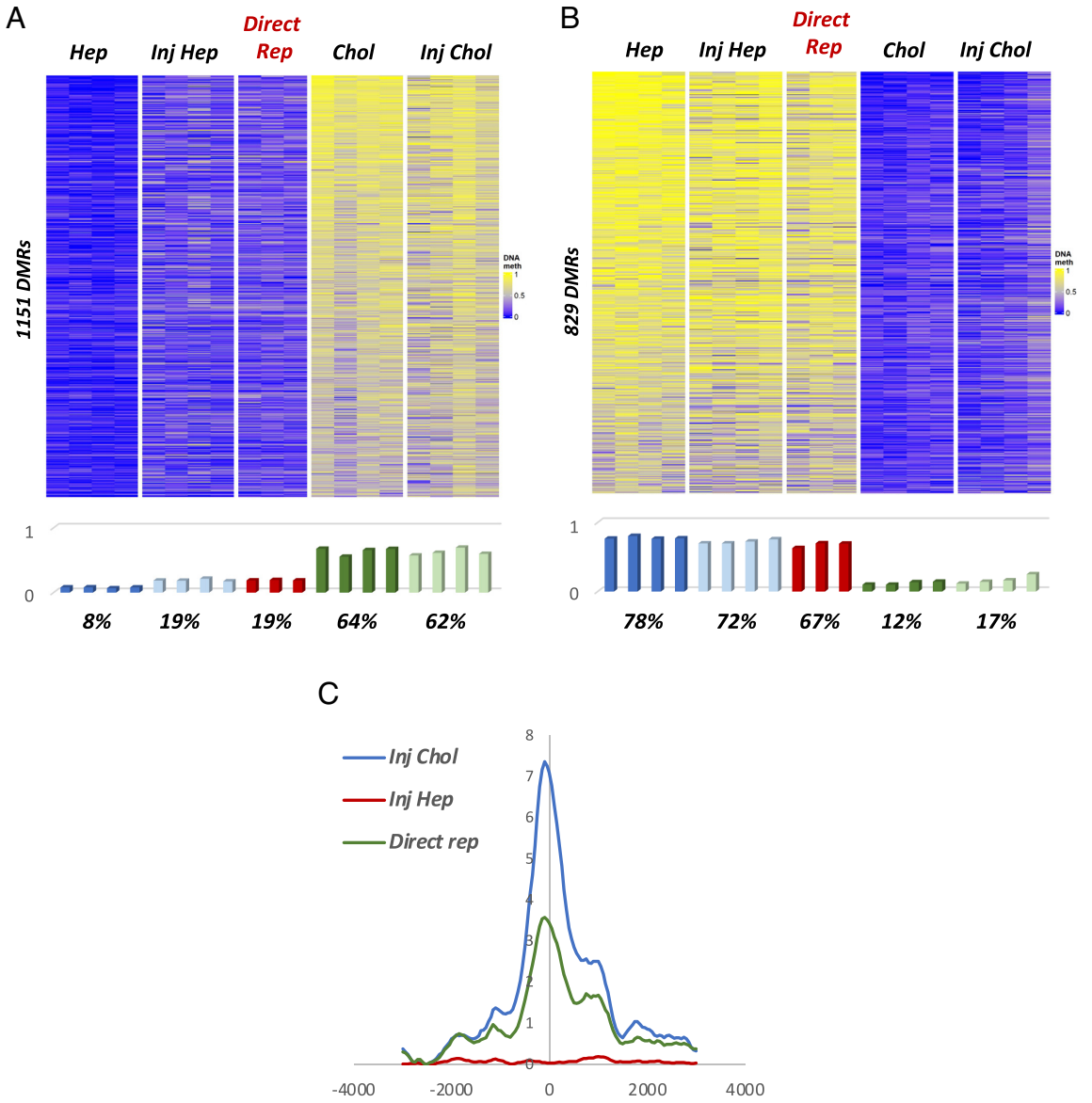

Fig. 3. Direct reprogramming from hepatocytes to cholangiocytes in vivo. Heatmap and histogram (average RRBS methylation for each sample) of specifically unmethylated regions in normal (Hep) or DDC-treated (Inj Hep) hepatocytes but not in cholangiocytes (*A*) or in normal (Chol) or DDC-treated (Inj Chol) cholangiocytes but not in hepatocytes (*B*) as compared to the pattern seen in reprogrammed cells (Direct Rep). (*C*) ATAC-Seq of cholangiocyte-specific undermethylated regions as determined by RRBS as a function of distance from their center.

developmentally oriented two-step pathway, first backconverting MEFs into pluripotent stem cells (iPSCs) and then differentiating them into neural precursors in vitro (see *Materials and Methods* for details). In contrast to our results following direct MEF-to-neuron transdifferentiation, the NPCs that arose via this two-step process exhibited a methylation pattern that strongly resembled bona fide NPCs, including demethylation of NPC-specific regulatory sites (*SI Appendix*, Fig. S4). This approach was evidently successful because it takes advantage of pre-existing developmentally programmed pathways to first dedifferentiate to pluripotency and then redifferentiate to a stable neuronal cell type (16).

Discussion

DNA Methylation Programming During Development. It is well established that fully differentiated somatic cells can be reprogrammed by artificially inducing a set of key transcription factors that can bring about pluripotency, similar to what is present in the pluripotent early embryo and these iPS cells can then serve as founders for full development. This reprogramming also takes place at the epigenetic level, with all the tissue-specific regulatory regions from the founder cell becoming remethylated. This is made possible because embryonic stem cells retain the active programming instructions and machinery that is employed during normal embryonic development to reset the gamete-derived genomic pattern in each individual and this represents an inherent feature of pluripotency (12). This ability to reset DNA methylation patterns, however, does not seem to be operative in any of the various examples of transdifferentiation tested in this study, either in vitro or in vivo.

All genes are influenced by multiple domain-wide regulatory elements that interact in 3D space with their promoter, thereby affecting expression (38). Development is primarily driven by interactions between protein factors and these cis-acting DNA sequences, and many studies have demonstrated that these transient molecular "decisions" are then stabilized by programmed changes in DNA methylation. Induction of gastrulation, for example, including the transcriptional repression of pluripotency genes

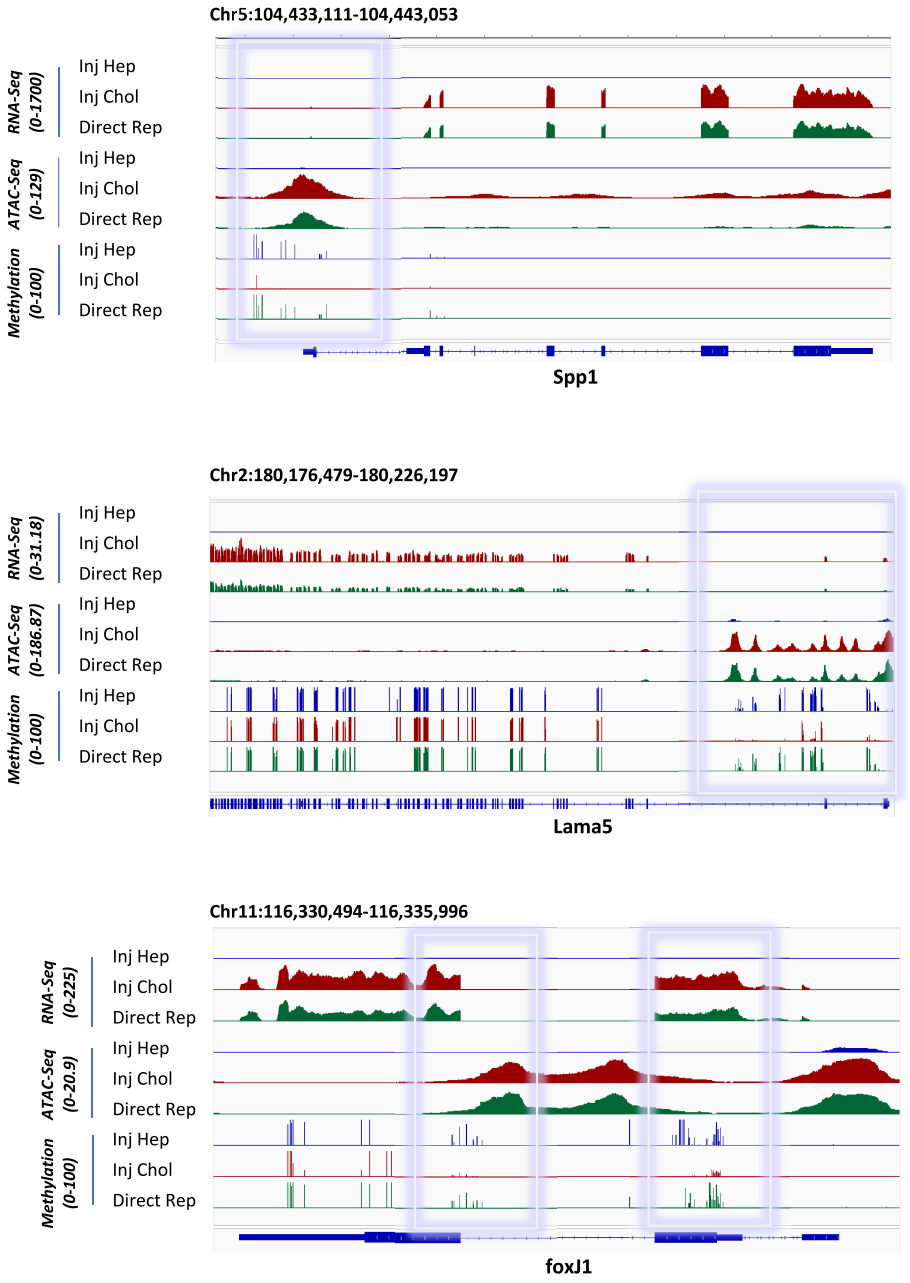

Fig. 4. Examples of genes with specifically undermethylated enhancer regions in cholangiocytes. Genome browser tracks showing RNA-Seq, ATAC-Seq, and DNA methylation of genes specifically expressed in cholangiocytes for DDC-treated hepatocytes (Inj Hep) or cholangiocytes (Inj Chol) as compared to reprogrammed cells (Direct Rep). The undermethylated regions are outlined in gray.

(e.g., *Oct4*), is initially accomplished by factor–DNA interactions, but if the subsequent de novo methylation step is inhibited, the newly differentiated phenotype is unstable and thus can readily revert back to the pluripotent state (21, 22). In other cases, inhibition of targeted demethylation or de novo methylation during lineage development generates only partial expression patterns that can then disrupt the proper differentiation of downstream cell types (39–42). It is this concept of methylation-pattern-induced stability that appears to underlie our findings. In all the cases studied, the factors used to induce transdifferentiation proved incapable of reprogramming DNA methylation patterns and, as a consequence, the resulting cell types, where tested, exhibited transient aberrant expression patterns and ultimately reverted back to their initial cell identity or underwent hypertrophy (17–19).

Our studies and others clearly show that reprogramming of terminally differentiated cells can be accomplished in a relatively simple manner by inducing high concentrations of master transcription factors such as MyoD that may act as an organizer (43) to set in motion the entire network of cell-type-specific gene expression with its accompanying alterations in chromatin structure (see legend to *SI Appendix*, Fig. S3). In contrast, methylation reprogramming appears to be more complicated and depends on built-in ratchet-like programming rules. As opposed to the kinetic protein–DNA interactions responsible for transcription regulation, targeted changes in DNA methylation are of a covalent nature and therefore stably maintained in both dividing and nondividing cells. It appears that it is these directionality rules that underlie the Waddington model at the molecular level.

Reprogramming in Medicine. These results have clear-cut implications regarding the use of reprogramming for tissue replacement in man. As has been previously reported, transdifferentiation does not manifest the full spectrum of their endogenous counterparts (17, 20) raising the question of whether this is a viable approach for replacement therapy. Our studies suggest that it is the DNA methylation profiles that are responsible for phenotypic stability and these fixed patterns cannot easily be modified without going through earlier stages of development where these patterns were originally established (44). It is important to emphasize that our findings should not be conflated with the occasional somatic memory observed in iPSCs. Unlike the memories observed in iPSCs, which do not impact cell identity and stability and occur in only a handful of loci, the aberrant methylation patterns identified in our study within transdifferentiated cells represent a widespread phenotype. These methylation changes span across many developmental-related loci, all of which are critical for the identity of the cells. However, once more is known about the factors and motifs that play a role in the normal in vivo programming of tissue-specific DNA methylation patterns, it should be possible to devise new molecular strategies for effective and stable transdifferentiation.

Materials and Methods

Experimental Design. The study aimed to explore why transdifferentiated cells don't fully recapitulate the function and activity of their endogenous counterparts. Recognizing the importance of DNA methylation in establishing cell identity, we developed a unique approach to analyze specific changes in DNA methylation associated with developmentally critical loci before and after transdifferentiation occurred. We studied two well-established in vitro transdifferentiation models–fibroblast to myofibroblast and fibroblast to neuron–as well as an in vivo model of transdifferentiation from hepatocytes to cholangiocytes following injury.

Cell Culture. MEFs were isolated as previously described (45). MEFs were grown in DMEM supplemented with 10% FBS, 2 mM L-glutamine, and antibiotics. iPSCs were grown in DMEM supplemented with 15% FBS, 1% nonessential amino acids, 2 mM L-glutamine, in-house mouse Leukemia inhibitory factor (mLif), 0.1 mM b-mercaptoethanol (Sigma), and antibiotics with or without 2i- PD0325901 (1 mM) and CHIR99021 (3 mM) (Tocris). For primary infection, Oct4-GFP MEFs were isolated from mice heterozygous for the reverse tetracycline-dependent transactivator (M2rtTA) that resides in the ubiquitously expressed Gt(ROSA)26Sor locus. All infections were performed on MEFs (passage 0 or 1) that were seeded at 80% confluency 2 d prior to the first infection The Joint Ethics Committee (IACUC) of the Hebrew University and Hadassah Medical Center approved the study protocol for animal welfare. The Hebrew University is an AAALAC international accredited institute.

Lentiviral infection–transdifferentiation of MEFs to myotubes. For infection, replication-incompetent lentiviruses containing the various reprogramming factors (OSKM, MyoD) were packaged with a lentiviral packaging mix (7.5 μg psPAX2 and 2.5 μg pGDM.2) in 293T cells and collected 48 h after transfection. The supernatants were filtered through a 0.45-μm filter, supplemented with 8 μg/mL of polybrene (Sigma), and then used to infect MEFs. To induce myogenic transdifferentiation, MyoD-transduced MEFs were exposed to fresh DMEM supplemented with heat-inactivated 2% horse serum, 2 μg/mL doxycycline, and 1% penicillin and streptomycin. Myotubes were then collected by a brief centrifugation 250×*g* for 1 min.

Differentiation of iPSCs into neurons. To induce neuron differentiation from iPSCs, embryoid bodies were cultured in hanging drops at 37 °C, 5% CO_2, for 4 d and then treated with all trans-RA (Sigma) for the next 4 d. After 4 d of suspension culture, the embryoid bodies were transferred to Poly-D-Lysine-coated cell culture dishes with neuronal medium containing N2 and B27 and cultured for 9 d.

Mice. Male RosaYFP/YFP and Smad4fl/fl mice on mixed backgrounds were injected retro-orbitally at 4 wk of age with 2.5 × 1,011 viral particles of AAV8-TBG-Cre virus obtained from the Penn Vector Core. One week following injection, mice were fed 0.1% wt/wt DDC (3,5-diethoxycarbonyl-1,4-dihydrocollidine, Sigma-Aldrich) (Envigo) for 2 to 6 wk. Studies were conducted in accordance with NIH and University of Pennsylvania Institutional Animal Care and Use Committee guidelines.

Liver Cell Preparation. Control and DDC-treated livers were perfused with 40 mL of 1X HBSS, followed by 40 mL HBSS/1 mM EGTA, and 40 mL of HBSS/5 mM $CaCl_2$/40 μg/mL liberase. Following perfusion, livers were mechanically dissociated and incubated 15 min in HBSS with $CaCl_2$ and 400 μg/mL liberase at 37 °C. Digests were filtered (70 μm) to generate single-cell suspensions and pelleted at 300×*g*. Following isolation, cells were incubated for 15 min on ice in 10 mL ACK Lysing Buffer (Lonza, 10–548E) and then washed in HBSS/5% FBS and stained for flow.

Flow Cytometry. Cells were stained for 25 min on ice at 1:100 with antibodies to EpCAM (Biolegend 118225), CD31 (Biolegend 102418), CD45 (Biolegend 103114), and CD11b (Biolegend 101216) with TOPRO3 (1:2,000) for live/dead staining (Invitrogen T3605). Cells were strained through a 35-μm filter and sorted by FACSAria (Becton Dickinson).

Libraries. Total RNA was isolated using the Qiagen RNeasy kit. mRNA libraries were prepared using the SENSE mRNA-seq library prep kit V2 (Lexogen), and pooled libraries were sequenced on an Illumina NextSeq 500 platform to generate 75-bp single-end reads.

DNA was isolated from mouse hepatocytes or from snap-frozen mouse tissues and incubated in lysis buffer [25 mM Tris-HCl (pH 8), 2 mM ethylenediaminetetraacetic acid, 0.2% sodium dodecyl sulfate, 200 mM NaCl] supplemented with 300 μg/mL proteinase K (Roche) followed by phenol:chloroform extraction and ethanol precipitation and RRBS libraries were prepared and run on HiSeq 2500 (Illumina) using 100 bp paired-end sequencing.

Data Analysis, Statistics, and Reproducibility. All experiments in this study have at least two independent replicates.

Low-quality bases and sequencing adaptors of raw fastq files RNA-seq containing single-end 61 bp-long reads were trimmed using Trim Galore (V 0.6.0, https://github.com/FelixKrueger/TrimGalore) and then mapped to the mm10 reference genome using HISAT2 (V 2.1.0) with default parameters. Read counting was performed using featureCounts (V 1.6.2) with mm10 gtf annotation. Differential gene expression analysis was performed using DESeq2 R package (V 1.26.0).

Demultiplexed reads from both published RRBS (GSE155111) and WGBS (GSE111283) were trimmed using Trim Galore (V 0.6.0, https://github.com/FelixKrueger/TrimGalore). Reads were then aligned to the mouse mm10 genome using BISulfite-seq CUI Toolkit (BISCUIT). Briefly, mm10 genome was indexed using the biscuit index command from biscuit. Reads were aligned using the biscuit align command and the output was sorted using the "sort" command from "samtools" package. A pileup VCF of DNA methylation and genetic information was then generated using the biscuit pileup command. DNA methylation BED data were then extracted using the biscuit vcf2bed command. Next, a wrapper function was used to convert methylation data from Biscuit to Methylkit acceptable format.

RRBS data were trimmed and quality filtered by trim galore software (v.0.3.3) using default parameters for RRBS. Read alignment (genome build mm10) and extraction of single-base resolution methylation levels were carried out by BSMAP v.2.74.

The resulting bed files were then converted to binary formatted beta files and the genome then segmented into 5,009,987 blocks using all our WGBS beta samples as reference. For RRBS segments, we first created a pseudo RRBS genome containing only the CpG sites found in all RRBS beta samples and segmented this RRBS genome into 446,860 blocks using all our RRBS samples as reference (wgbstools package with default values set at pseudocount 15 and min CpG 1).

We calculated hypodifferentially methylated segments (DMRs) between target tissue samples and other tissue samples using the wgbstools find_markers command by specifying that only segments with a minimum coverage of 10 CpGs, a P-value < 0.01 (T test), and whose quantiles satisfied '--delta_quants 0.4 --tg_quant 0 --bg_quant 0.5'--delta_means:0.4--delta_quants:0.0--tg_quant: 0--bg_quant:0.5--unmeth_quant_thresh:0.4--meth_quant_thresh:0.6--unmeth_mean_thresh:1.0--meth_mean_thresh:0.0--. Next, by using the wgbstools beta_to_table command, we generated a table of methylation scores for all the samples that appear in the heatmap figures in each of the calculated

DMR segments. The DMRs presented in the heatmaps are those with at least 30% difference between the two cell types of interest (MEF/muscle, MEF/NPC, Hep/BEC).

Data, Materials, and Software Availability. Sequencing data have been deposited in the GEO under Accession No. GSE252355 (46). The data that support the findings of this study are available from the corresponding author upon reasonable request. All other data are included in the manuscript and/or *SI Appendix*.

ACKNOWLEDGMENTS. This study was supported by Israel Science Foundation grants to Y.B. (161/23) and H.C. (1578/20), the NIH (2R01DK083355 to B.Z.S.), the European Molecular Biology Organization (EMBO) Young Investigator Programme (to Y.B.), the Israel Cancer Research Foundation (to H.C.), The Fred and Suzanne Biesecker Pediatric Liver Center (B.Z.S.), and a generous gift from Ms. Nadia Guth Biasini. We also thank Allyson Merrell.

Author affiliations: [a]Department of Developmental Biology and Cancer Research, Institute for Medical Research Israel-Canada, Hebrew University Medical School, Jerusalem 91120, Israel; [b]Department of Medicine and Cell, The Institute for Regenerative Medicine, Perelman School of Medicine at the University of Pennsylvania, Philadelphia, PA 19104; and [c]Department of Development Biology, The Institute for Regenerative Medicine, Perelman School of Medicine at the University of Pennsylvania, Philadelphia, PA 19104

1. C. H. Waddington, *The Strategy of Genes* (George Allen and Unwin, London, UK, 1957).
2. H. Cedar, Y. Bergman, Programming of DNA methylation patterns. *Annu. Rev. Biochem.* **81**, 97–117 (2012).
3. T. Kafri *et al.*, Developmental pattern of gene-specific DNA methylation in the mouse embryo and germ line. *Genes Dev.* **6**, 705–714 (1992).
4. M. Monk, M. Boubelik, S. Lehnert, Temporal and regional changes in DNA methylation in the embryonic, extraembryonic and germ cell lineages during mouse embryo development. *Development* **99**, 371–382 (1987).
5. M. Brandeis *et al.*, Sp1 elements protect a CpG island from de novo methylation. *Nature* **371**, 435–438 (1994).
6. D. Frank *et al.*, Demethylation of CpG islands in embryonic cells. *Nature* **351**, 239–241 (1991).
7. R. Greenfield *et al.*, Role of transcription complexes in the formation of the basal methylation pattern in early development. *Proc. Natl. Acad. Sci. U.S.A.* **115**, 10387–10391 (2018).
8. Y. Dor, H. Cedar, Principles of DNA methylation and their implications for biology and medicine. *Lancet* **392**, 777–786 (2018).
9. J. B. Gurdon, The developmental capacity of nuclei taken from intestinal epithelium cells of feeding tadpoles. *J. Embryol. Exp. Morphol.* **10**, 622–640 (1962).
10. I. Wilmut, A. E. Schnieke, J. McWhir, A. J. Kind, K. H. Campbell, Viable offspring derived from fetal and adult mammalian cells. *Nature* **385**, 810–813 (1997).
11. K. Takahashi, S. Yamanaka, Induction of pluripotent stem cells from mouse embryonic and adult fibroblast cultures by defined factors. *Cell* **126**, 663–676 (2006).
12. O. Sabag *et al.*, Establishment of methylation patterns in ES cells. *Nat. Struct. Mol. Biol.* **21**, 110–112 (2014).
13. T. Graf, T. Enver, Forcing cells to change lineages. *Nature* **462**, 587–594 (2009).
14. H. Shelby, T. Shelby, M. Wernig, Somatic lineage reprogramming. *Cold Spring Harb. Perspect. Biol.* **14**, a040808 (2022).
15. A. J. Merrell, B. Z. Stanger, Adult cell plasticity in vivo: De-differentiation and transdifferentiation are back in style. *Nat. Rev. Mol. Cell Biol.* **17**, 413–425 (2016).
16. P. Cahan *et al.*, Cell Net: Network biology applied to stem cell engineering. *Cell* **158**, 903–915 (2014).
17. B. D. Tarlow *et al.*, Bipotential adult liver progenitors are derived from chronically injured mature hepatocytes. *Cell Stem Cell* **15**, 605–618 (2014).
18. M. Yagi *et al.*, Dissecting dual roles of MyoD during lineage conversion to mature myocytes and myogenic stem cells. *Genes Dev.* **35**, 1209–1228 (2021).
19. K. Hiramatsu *et al.*, Generation of hyaline cartilaginous tissue from mouse adult dermal fibroblast culture by defined factors. *J. Clin. Invest.* **121**, 640–657 (2011).
20. S. Sebban, Y. Buganim, Nuclear reprogramming by defined factors: Quantity versus quality. *Trends Cell Biol.* **26**, 65–75 (2016).
21. N. Feldman *et al.*, G9a-mediated irreversible epigenetic inactivation of Oct-3/4 during early embryogenesis. *Nat. Cell Biol.* **8**, 188–194 (2006).
22. S. Epsztejn-Litman *et al.*, De novo DNA methylation promoted by G9a prevents reprogramming of embryonically silenced genes. *Nat. Struct. Mol. Biol.* **15**, 1176–1183 (2008).
23. H. M. Blau *et al.*, Plasticity of the differentiated state. *Science* **230**, 758–766 (1985).
24. E. C. Hardeman, C. P. Chiu, A. Minty, H. M. Blau, The pattern of actin expression in human fibroblast x mouse muscle heterokaryons suggests that human muscle regulatory factors are produced. *Cell* **47**, 123–130 (1986).
25. A. B. Lassar, B. M. Paterson, H. Weintraub, Transfection of a DNA locus that mediates the conversion of 10T1/2 fibroblasts to myoblasts. *Cell* **47**, 649–656 (1986).
26. S. J. Tapscott *et al.*, MyoD1: A nuclear phosphoprotein requiring a Myc homology region to convert fibroblasts to myoblasts. *Science* **242**, 405–411 (1988).
27. P. Boyle *et al.*, Gel-free multiplexed reduced representation bisulfite sequencing for large-scale DNA methylation profiling. *Genome Biol.* **13**, R92 (2012).
28. G. C. Hon *et al.*, Epigenetic memory at embryonic enhancers identified in DNA methylation maps from adult mouse tissues. *Nat. Genet.* **45**, 1198–1206 (2013).
29. C. Luo *et al.*, Global DNA methylation remodeling during direct reprogramming of fibroblasts to neurons. *eLife* **8**, e40197 (2019).
30. T. Vierbuchen *et al.*, Direct conversion of fibroblasts to functional neurons by defined factors. *Nature* **463**, 1035–1041 (2010).
31. K. Yanger *et al.*, Robust cellular reprogramming occurs spontaneously during liver regeneration. *Genes Dev.* **27**, 719–724 (2013).
32. J. R. Schaub *et al.*, De novo formation of the biliary system by TGFβ-mediated hepatocyte transdifferentiation. *Nature* **557**, 247–251 (2018).
33. A. J. Merrell *et al.*, Dynamic transcriptional and epigenetic changes drive cellular plasticity in the liver. *Hepatology* **74**, 444–457 (2021).
34. M. Naama *et al.*, Pluripotency-independent induction of human trophoblast stem cells from fibroblasts. *Nat. Commun.* **14**, 3359 (2023).
35. M. Jaber *et al.*, Comparative parallel multi-omics analysis during the induction of pluripotent and trophectoderm states. *Nat. Commun.* **13**, 3475 (2022).
36. J. M. Polo *et al.*, A molecular roadmap of reprogramming somatic cells into iPS cells. *Cell* **151**, 1617–1632 (2012).
37. Y. Buganim *et al.*, The developmental potential of iPSCs is greatly influenced by reprogramming factor selection. *Cell Stem Cell* **15**, 295–309 (2014).
38. L. A. Pennacchio, W. Bickmore, A. Dean, M. A. Nobrega, G. Bejerano, Enhancers: Five essential questions. *Nat. Rev. Genet.* **14**, 288–295 (2013).
39. Y. Reizel *et al.*, Postnatal DNA demethylation and its role in tissue maturation. *Nat. Commun.* **9**, 2040 (2018).
40. S. Orlanski *et al.*, Tissue-specific DNA demethylation is required for proper B-cell differentiation and function. *Proc. Natl. Acad. Sci. U.S.A.* **113**, 5018–5023 (2016).
41. A.-M. Bröske *et al.*, DNA methylation protects hematopoietic stem cell multipotency from myeloerythroid restriction. *Nat. Genet.* **41**, 1207–1215 (2009).
42. G. A. Challen *et al.*, Dnmt3a is essential for hematopoietic stem cell differentiation. *Nat. Genet.* **44**, 23–31 (2011).
43. R. Wang *et al.*, MyoD is a 3D genome structure organizer for muscle cell identity. *Nat. Commun.* **13**, 205 (2022).
44. T. Falick Michaeli *et al.*, Hepatocyte regeneration is driven by embryo-like DNA methylation reprogramming. *Proc. Natl. Acad. Sci. U.S.A.* **121**, e2314885121 (2024).
45. M. Wernig *et al.*, A drug-inducible transgenic system for direct reprogramming of multiple somatic cell types. *Nat. Biotechnol.* **26**, 916–924 (2008).
46. Ahmed Radwan, Jason Eccleston *et al.*, "Transdifferentiation occurs without resetting development-specific DNA methylation, a key determinant of full-function cell identity". GEO. https://www.ncbi.nlm.nih.gov/geo/query/acc.cgi?acc=GSE252355. Deposited 2 January 2024.